

SOL – GEL PREPARATION OF A DI-UREASIL ELECTROLYTE DOPED WITH LITHIUM PERCHLORATE

M. M. Silva^{*a}, S. C. Nunes^b, V. de Zea Bermudez^b, P. C. Barbosa^a, A. Evans^a
M. J. Smith^a and D. Ostrovskii^c

^aDepartamento de Química, Universidade do Minho, Gualtar, 4710-057 Braga, Portugal

^bDepartamento de Química and CQ-VR, Universidade de Trás-os-Montes e Alto Douro,
5000-911 Vila Real, Portugal

^cDepartment of Applied Physics, Chalmers University of Technology, 41296 Goteborg,
Sweden.

*nini@quimica.uminho.pt

Abstract

Solid polymer electrolytes (SPEs) synthesized by the sol-gel process and designated as ormolytes (organically modified electrolytes), have been prepared through the incorporation of lithium perchlorate, LiClO₄ into the U(2000) organic-inorganic hybrid network. Electrolytes with lithium salt compositions of n (where n indicates the number of oxyethylene units per Li⁺ ion) between ∞ and 0.5 were characterized by conductivity measurements, cyclic voltammetry at a gold microelectrode, thermal analysis and spectroscopic techniques. The conductivity results obtained suggest that this system offers a quite significant improvement over previously characterized analogues doped with lithium triflate [1].

1. Introduction

The genesis of solvent-free SPEs is generally considered to have taken place in 1973 with the publication of the study of a poly(ethylene oxide), PEO-based system by Fenton and co-workers [2]. Recognition of the potential application of these semi-crystalline solids in advanced batteries [3, 4] naturally led to a rapid increase of interest and the production of a large number of publications that have formed the foundation of this sub-domain of the solid electrolyte class of materials [5-10]. Although applications

have been proposed in sensors, displays, intelligent windows and reactive labels, the main impetus of research continues to be directed toward advanced batteries.

First-generation SPEs were based on commercial poly(ethylene oxide) but it was soon realized that the performance limitation imposed by the crystalline component of this macromolecule could be attenuated by using amorphous PEO-derived synthetic networks. Many examples can be found of new electrolytes based on co-polymers [11] and blends [12], materials doped with nano-dimensioned fillers [13] or plasticized formulations [10]. In the search for novel host networks a promising strategy is provided by the application of the sol-gel process [14, 15] to produce organic-inorganic hybrid networks. This synthetic approach allows networks with tailored physical and chemical properties to be produced without recourse to complex experimental procedures.

In this study we report the synthesis of a hybrid network electrolyte, designated as a di-ureasil [16-18], which has been doped with controlled quantities of LiClO_4 . The oxyethylene segments of a commercial diamine were incorporated into a silica matrix through urea bridges to form a network with encouraging chemical, electrochemical and mechanical properties. The resulting macromolecular structures also show high optical transparency, good thermal stability and are completely amorphous.

2. Experimental Details

2.1. Materials

Lithium perchlorate (Aldrich, 99,99%) and α,β -diaminepoly(oxyethylene-co-oxypropylene (commercially available as Jeffamine ED-2001®, Fluka, average molecular weight 2001 gmol^{-1}) were dried under vacuum at 25 °C for several days prior to use. The bridging agent, 3-isocyanatepropyltriethoxysilane (ICPTES, Aldrich 95 %) was used as received. Ethanol (Merck, 99,8%) and tetrahydrofuran (Merck, 99,9%) were dried over molecular sieves prior to use. High purity distilled water was used in all experiments.

2.2. Synthesis

The LiClO_4 -based di-ureasils were prepared according to an optimized two-step method described in detail elsewhere [1]. The synthetic procedure involved grafting a diamine containing oxyethylene units to the isocyanatepropyltriethoxysilane precursor, to yield

the di-urea (-NH(C=O)NH-) cross-linked hybrid precursor. This material was subsequently hydrolyzed and condensed in the sol-gel stage of the synthesis to induce the growth of the siloxane network.

Step 1 - Synthesis of the di-ureasil precursor, d-UPTES(2000): 2.0 g of Jeffamine 2001 were dissolved in 10 ml of THF with stirring. A volume of 494 μl of ICPTES was added to this solution in a fume cupboard (molar proportion 1 Jeffamine 2001: 2 ICPTES). The flask was then sealed and the solution stirred for about 12 h at moderate temperature ($\approx 40\text{ }^\circ\text{C}$). A urea cross-linked organic/inorganic material, designated as di-ureapropyltriethoxysilane (d-UPTES(2000)), was obtained under these conditions. The grafting process was followed by infrared monitoring. During this reaction the intensity of the isocyanate vibrational band situated at approximately 2273 cm^{-1} progressively decreased, finally disappearing when the reaction was complete. These spectral changes were accompanied by the growth of a series of bands due to the presence of urea groups in the region between 1800 and 1500 cm^{-1} .

Step 2 - Synthesis of the di-ureasil xerogels, d-U(2000)_nLiClO₄: A volume of 466 μl of $\text{CH}_3\text{CH}_2\text{OH}$, an appropriate mass of LiClO_4 (see Table 1) and 54 μl of water were added to the d-UPTES(2000) solution prepared in the previous step (molar proportion 1 ICPTES: 4 $\text{CH}_3\text{CH}_2\text{OH}$: 1.5 H_2O). The mixture was stirred in a sealed flask for approximately 30 min and then cast into a Teflon mould, covered with Parafilm and stored in a fume cupboard for 24 h. The mould was transferred to an oven at $50\text{ }^\circ\text{C}$ and the sample was aged for a period of 4 weeks.

In agreement with the terminology adopted in previous publications [16-18], the ormolytes were identified using the notation $\text{d-U}(2000)_n\text{LiClO}_4$. In this representation the $\text{d-U}(2000)$ denotes the presence of the host di-ureasil framework with average molecular weight of 2000 and n expresses the salt content in terms of the number of ether oxygen atoms per Li^+ cation.

The xerogels with n greater than 5 were obtained as flexible transparent, monolithic films with a yellowish hue whereas the compounds with $n = 1$ and 0.5 were rather brittle, powdery agglomerates. The content of LiClO_4 in selected samples and other relevant information is included in Table 1.

2.3. Experimental techniques

FT-Raman spectroscopy. The FT-Raman spectra were recorded at room temperature with a Bruker IFS-66 spectrometer equipped with a FRA-106 Raman module and a near-infrared YAG laser with wavelength 1064 nm. The spectra were collected over the 3200-300 cm^{-1} range at a resolution of 2 cm^{-1} . The accumulation time for each spectrum was 4 hours.

The iterative least-squares curve-fitting procedure in PeakFit [19] software was used extensively throughout this study. The best fit of the experimental data was sought by varying the frequency, bandwidth and intensity of the bands. The standard errors of the curve-fitting procedure were less than 0.002. In this study of LiClO_4 -doped di-ureasils the best fit of spectral data was obtained by using a mixture of Lorentzian and Gaussian contributions.

Ionic conductivity. The total ionic conductivity of the ormolyte was determined by locating an electrolyte disk between two 10 mm diameter ion-blocking gold electrodes (Goodfellow, > 99.95%) to form a symmetrical cell. The electrode/ormolyte/electrode assembly was secured in a suitable constant volume support [20] and installed in a Buchi TO51 tube oven. A type K thermocouple was placed close to electrolyte disk to measure the sample temperature. Bulk conductivities of electrolyte samples were obtained during heating cycles using the complex plane impedance technique (Schlumberger Solartron 1250 frequency response analyzer and 1286 electrochemical interface) between 25 and 100 $^{\circ}\text{C}$ and at approximately 7 $^{\circ}\text{C}$ intervals.

Thermal analysis. Ormolyte sections were removed from dry films and subjected to thermal analysis under a flowing argon atmosphere between 40 and 350 $^{\circ}\text{C}$ and at a heating rate of 5 $^{\circ}\text{C}\cdot\text{min}^{-1}$ using a Mettler DSC 821e. Samples were transferred to 40 μL aluminium cans with perforated lids within a dry argon-filled glovebox. Samples for thermogravimetric studies were prepared in a similar manner, transferred to open crucibles and analyzed using a Rheometric Scientific TG1000 thermobalance operating under a flowing argon atmosphere. A heating rate of 10 $^{\circ}\text{C}\cdot\text{min}^{-1}$ was used with all samples.

Electrochemical stability. Evaluation of the electrochemical stability window of electrolyte compositions was carried out within a dry argon-filled glovebox using a two-electrode cell configuration. The preparation of a 25 μm diameter gold microelectrode surface by the conventional polishing routine was completed outside the drybox. The microelectrode was then washed with THF, dried with a hot-air blower and transferred to the drybox. The cell assembly was initiated by locating a clean lithium disk counter

electrode (Aldrich, 99.9%, 10 mm diameter, 1mm thick) on a stainless steel current collector. A thin-film sample of electrolyte was centered over the counter electrode and the cell assembly completed by locating and supporting the microelectrode in the centre of the electrolyte disk. The assembly was held together firmly with a clamp and electrical contacts were made to the Autolab PGSTAT-12 (Eco Chemie) used to record voltammograms at a scan rate of 100mVs^{-1} . Measurements were conducted at room temperature within a Faraday cage located inside the measurement glovebox.

3. Results and Discussion

3.1 - Cation/anion interactions

Raman spectroscopy is a technique that has been extensively applied in the study of interactions between cations and anions and the identification of the charge carriers present in electrolytes. The concentration and nature of charge carriers may be expected to influence the total ionic conductivity of hybrid PEO/siloxane systems. In general the ionic species present in conventional polymer electrolytes can be classified as: (1) “free” or weakly-coordinated ions with high mobility; (b) solvent-separated ion pairs and contact ion pairs with moderate mobility; (c) triplet ion clusters and higher order ionic aggregates with low mobility. High total ionic conductivity is expected to be a consequence of a higher percentage of salt dissociation and therefore enhanced mobility in the electrolyte.

The ClO_4^- anion is an excellent spectral probe that allows the extent of ionic association to be evaluated. This anion has a tetrahedral symmetry and the nine vibrational degrees freedoms are distributed into four normal modes: $\nu_1(\text{A}_1)$, $\nu_2(\text{E})$, $\nu_3(\text{T}_2)$ and $\nu_4(\text{T}_2)$ [21-22]. Useful information regarding the behaviour of the $\text{d-U}(2000)_n\text{LiClO}_4$ electrolyte system may therefore be obtained through the analysis of the FT-Raman non-degenerate symmetric stretching vibration mode of the ClO_4^- anion, $\nu_1(\text{A}_1)$. The $\nu_1\text{ClO}_4$ band of a “free” ClO_4^- was located around $933\text{-}930\text{ cm}^{-1}$ [23-30]. Upon coordination, the $\nu_1(\text{A}_1)$ band was found to shift to higher wavenumbers [23-30]. The FT-Raman spectra and the results of the curve-fitting carried out in the FT-Raman $\nu_1\text{ClO}_4$ band profiles of selected LiClO_4 -based di-ureasils are represented in Fig. 1(a) and (b). The variation of the integral area fraction of the isolated components with composition is shown in Fig. 2 and the relevant data is collected in Table 2.

Fig. 1 demonstrates that in the $d\text{-U}(2000)_n\text{LiClO}_4$ hybrids with $n \geq 5$ the intensity maximum of the FT-Raman $\nu_1\text{ClO}_4$ envelope appears at 930 cm^{-1} . With an increase in salt concentration (to $n = 5$) the intensity maximum of this band shifts to 932 cm^{-1} , whereas in di-ureasils with even greater salt content, at $n = 1$ and 0.5 , the maximum is observed at about $935\text{-}936\text{ cm}^{-1}$.

The FT-Raman $\nu_1\text{ClO}_4$ envelope of the Li^+ -based $d\text{-U}(2000)$ doped hybrids with $n \geq 40$ was decomposed into three components: two bands at $930\text{-}931$ and $909\text{-}910\text{ cm}^{-1}$ and a shoulder at $924\text{-}926\text{ cm}^{-1}$ (Fig. 1(a)). In the range of salt concentration $25 \geq n \geq 5$ a new shoulder develops at $935\text{-}936\text{ cm}^{-1}$ (Figs. 1(a) and 1(b)). At $n \geq 5$ the relative intensity of the three components remains practically unchanged (Figs. 1(a) and 1(b), Table 2). In the FT-Raman $\nu_1\text{ClO}_4$ envelope of the most concentrated di-ureasils studied ($n = 1$ and 0.5) the $935\text{-}936\text{ cm}^{-1}$ event becomes the most intense feature of this region (Fig. 1(b) and Table 2). Finally, at $n = 0.5$ a new shoulder emerges at 941 cm^{-1} (Fig. 1(b) and Table 2). The $930\text{-}931\text{ cm}^{-1}$ band, which remains at the same position in all the FT-Raman spectra irrespective of the salt concentration, is assigned to “free” ions [23-30]. The shoulder at $924\text{-}926\text{ cm}^{-1}$, present in the FT-Raman spectra of all the samples analyzed, has only been reported in the literature by Brooker et al. [30] who assigned it to a $2\nu_2\text{ClO}_4$ mode. We will leave this mode unassigned. The weak event located at $909\text{-}910\text{ cm}^{-1}$ observed in the FT-Raman spectra of the Li^+ -doped di-ureasils with $n = 40, 25, 10$ and 5 is associated with the first overtone of the $\nu_2(\text{E})$ deformation mode of the ClO_4^- ion (i.e., $2\nu_2\text{ClO}_4$) [23, 26, 27, 29]. The 936 cm^{-1} feature seen in the FT-Raman spectra of samples with $n = 10, 5, 1$ and 0.5 is ascribed to contact ion-pairs mono-dentally coordinated ($\text{Li}^+ \text{- ClO}_4^-$). By this affirmation we mean that there is at least one direct coordination of the Li^+ ion to one perchlorate oxygen [23-30]. The broad higher frequency component at 941 cm^{-1} found at $n = 0.5$ indicates the presence of higher order ionic aggregates [24, 28].

Based on these spectral assignments, and the variation of peak integral area fraction with electrolyte composition, analysis of the data presented in Table 2 and Figure 2, suggests that free ion concentration decreases between about $n = 10$ and 0.5 and contact ion pair concentration increases over the same composition range. Spectral evidence also indicates that higher ion aggregate concentration increases at compositions with n less than about 5 .

3.2 - Electrochemical behaviour of the $d\text{-U}(2000)_n\text{LiClO}_4$ electrolytes

Conductivity Measurements

The choice of lithium perchlorate as the guest species in this electrolyte results in an improvement relative to systems based on other salts with a lower tendency to dissociate. The materials characterized in this study show a non-linear variation of ionic conductivity with temperature in the range between 25 and 100 °C (Fig. 3(a) and 3(b)). This behaviour is often observed with amorphous polymer electrolytes. The resulting conductivity isotherms are illustrated in Fig. 4 and confirm that ionic transport in the hybrid $\text{U}(2000)_n\text{LiClO}_4$ electrolyte system is almost independent of the salt content over a fairly wide range of composition of between $n = 40$ and 5. This figure also confirms the presence of a conductivity maxima at $n = 20$ at moderate temperatures. This observation is consistent with the suggestion, based on spectral evidence, that the number of charge carriers increases with salt content from $n = 200$ to an optimum composition over the range $n = 10$ to 20. Further increase in salt content results in a greater tendency for ionic association, the formation of ion aggregates and a decrease in total ionic conductivity [32-34]. At higher temperatures the difference in electrolyte performance is less and the composition range over which electrolytes support high conductivity is extended to $n = 5$.

It is probable that the existence of a range of electrolyte compositions with higher conductivity is a result of various factors. The dissociation of the guest salt into mobile ions is clearly important but the effect of the guest species on the glass transition temperature and mobility of the matrix segment is certainly also significant.

Thermal analysis

The DSC thermograms of electrolyte samples confirm that all the samples produced with compositions between $n = 0.5$ and 200 were completely amorphous. The temperature at which the onset of thermal decomposition (see Fig 5) occurs may effectively limit the application of a given electrolyte in a specific technological application. From previous studies of electrolytes with oxyethelene segments the consequence of an increase in salt content is expected to be a decrease in the onset of thermal degradation. The lowest decomposition temperature observed with the $d\text{-U}(2000)_n\text{LiClO}_4$ system is located at the $n = 20$ composition. Results obtained by DSC and thermogravimetric analysis are consistent with a minimum thermal stability of

235°C, a value considered acceptable for most foreseeable applications under normal operating conditions. Surprisingly, at even higher salt compositions the onset of thermal decomposition seems to increase.

The glass transition temperature or T_g of a polymer matrix is determined by chain segment flexibility and is taken as the temperature above which segmental motion begins. In the di-ureasil system the lowest T_g is associated with the composition of $n = 40$. The results obtained are included in Fig. 6. The value of T_g is also influenced by the intensity of interactions between polymer segments and the polymer and guest salt. As the salt content of the electrolyte is increased, the presence of polymer-salt interactions eventually restricts segmental mobility of the host polymer matrix and therefore at compositions of n lower than about $n = 20$ T_g increases and contributes to the observed decrease in ionic conductivity.

Electrochemical stability

The electrochemical stability of the lithium perchlorate and di-ureasil matrix electrolyte with composition $\text{di(U2000)}_{20}\text{LiClO}_4$ was determined by microelectrode cyclic voltammetry over the potential range 0V \rightarrow 7V. The stability limit for the electrolyte system was considered to be the potential at which a rapid rise in current was observed and where the current continued to increase as the potential was swept in the same direction. The overall stability of the electrolytes was excellent with no electrochemical oxidation occurring at anodic potentials less than about 5V. Figure 7 shows a typical voltammogram of an electrolyte sample of $\text{d(U2000)}_{10}\text{LiClO}_4$ composition. This data was recorded during the first scan from 0V to the anodic decomposition limit at between 4.5 and 5 V. The peak detected on the cathodic sweep at approximately 4.2 V and the poorly-resolved peaks at between 1.7 and 3 V were attributed to the reduction of decomposition products. The stability of this electrolyte is therefore considered adequate for application in lithium primary and secondary cells, a result in complete accordance with expectations from previous studies of oxyethylene-based electrolytes [23].

4. Conclusions

Ormolytes based on the U(2000) host and the guest LiClO_4 salt have been prepared by a simple synthetic procedure based on the sol-gel process. The advantage of this strategy is that fine-tuning of the mechanical properties of the matrix is fairly easily

accomplished by altering the synthetic conditions. The films obtained were homogeneous and completely amorphous over a wide range of salt composition. Their thermal and electrochemical stability is considered appropriate for a variety of technological applications and the total ionic conductivity observed is significantly better than networks doped with lithium triflate [1]. These electrolytes are transparent films with excellent mechanical properties that facilitate manipulation and the maintenance of good interfacial contacts. The preliminary studies of these hybrid networks suggest that exploitation of this strategy, with appropriate optimization of synthetic conditions and choice of adequate ionic guest species, may lead to the development of attractive electrolyte components for practical devices.

5. Acknowledgements

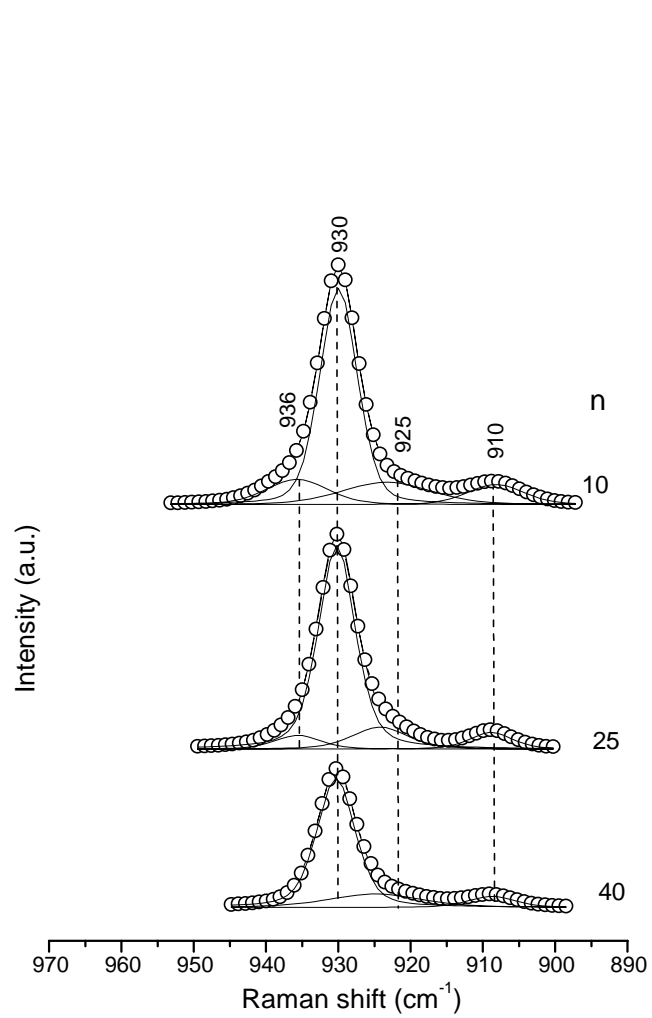
The authors are pleased to acknowledge the support provided by the Universities of Minho and UTAD, and the *Fundação para Ciência e Tecnologia* (contract POCI/QUI/59856/2004) for laboratory facilities and by the *Fundação Calouste Gulbenkian* for travel funds (MMS).

References

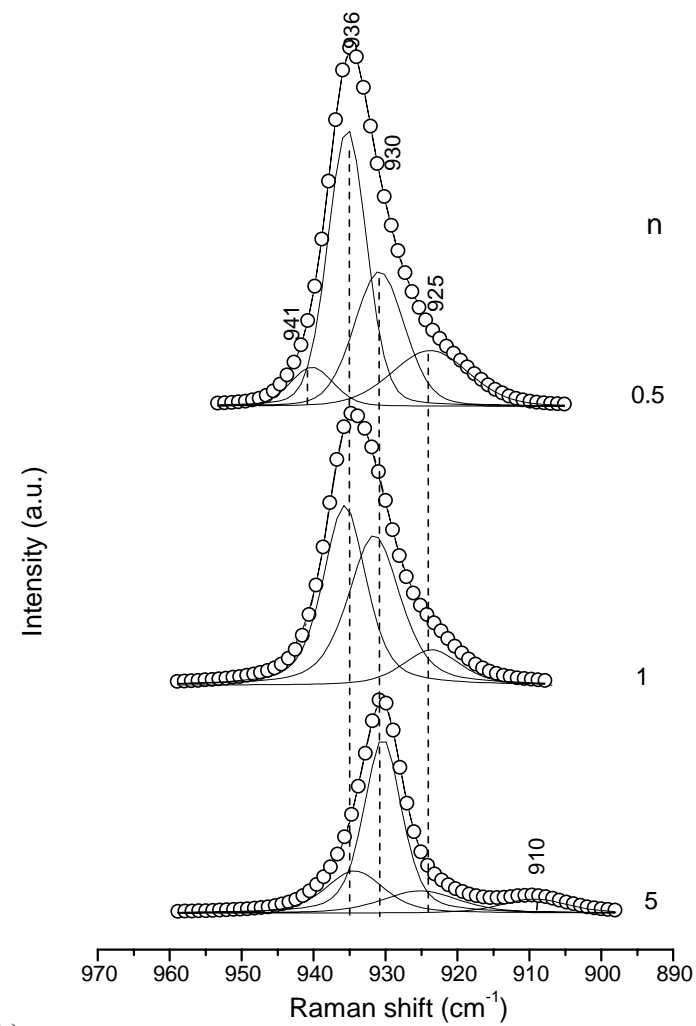
- [1] S. C. Nunes, V. de Zea Bermudez, D. Ostrovskii, M. M. Silva, S. Barros, M. J. Smith, R. A. Sá Ferreira, L. D. Carlos, J. Rocha, E. Morales, *J. Electrochem. Soc.*, 152(2) (2005), A429-A438
- [2] B. E. Fenton, J. M. Parker, P. V. Wright, *Polymer* 14, (1973) 589.
- [3] P. V. Wright, *Br. Polymer J.* 7, (1975) 319.
- [4] C. A. Vincent, *Chemistry in Britain*, (1989) 391.
- [5] M. Armand, *Faraday Discuss. Chem. Soc.* 88 (1989) 65-76.
- [6] M. B. Armand, J. M. Chabagno, M. Duclot, Second International Meeting on Solid Electrolytes, St. Andrews, Scotland, 20-22 Sept., 1978, Extended Abstract (1989).
- [7] M. B. Armand, J. M. Chabagno, M. J. Duclot, in: Proceedings of the Second International Conference on Solid Electrolytes, St. Andrews, Vol. 5, Paper 6, 1978 (Book of abstracts).
- [8] M. B. Armand, B. C. H. Steele, *Fast Ion Transport in Solids*, ed. W. Van Gool, North-Holland, New York, (1973).

- [9] a) F. M. Gray, in *Solid Polymer Electrolytes: Fundamentals and Technological Applications*, VCH Publishers, Inc. (1991); b) F. M. Gray, in *Polymer Electrolytes*, RSC Materials Monographs, Royal Society of Chemistry, London, (1997)
- [10] M. B. Armand, in *Polymer Electrolyte Reviews – 1* (Edited by J. R. MacCallum and C. A. Vincent), p. 1. Elsevier, London (1987).
- [11] T. Michot, A. Nishimoto, M. Watanabe, *Electrochimica Acta*, 45 (2000) 1347.
- [12] F. Chia, Y. Zheng, J. Liu, N. Reeves, G. Ungar, P. V. Wright, *Electrochimica Acta*, 48 (2003) 1939.
- [13] Seshumani Vorrey and Dale Teeters, *Electrochimica Acta*, 48 (2003) 2137.
- [14] C. J. Brinker, G. W. Scherer, *Sol-Gel Science: The Physics and Chemistry of Sol-Gel Processing*, Academic Press, San Diego, CA, (1990).
- [15] P. Gomez-Romero, C. Sanchez (Eds), *Functional Hybrid Materials*, Wiley Interscience, New York, (2003).
- [16] S. C. Nunes, V. de Zea Bermudez, M. M. Silva, S. Barros, M. J. Smith, E. Morales, L. D. Carlos, J. Rocha, *Solid State Ionics*, 176 (2005) 1591.
- [17] M. M Silva, V. de Zea Bermudez, L. D. Carlos, A. P. Passos de Almeida, M. J. Smith, *J. Mater. Chem.*, 9, 1735 (1999)
- [18] M. M. Silva, V. de Zea Bermudez, L. D. Carlos, M. J. Smith, *Electrochim. Acta*, 45, 1467 (2000)
- [19] PeakFit is a product of Jandel Corporation, 2591 Rerner Boulevard, San Rafael, CA 94901, U.S.A.
- [20] C. J. R. Silva, M. J. Smith, *Electrochimica Acta*, 40 (1995) 2389.
- [21] S. Ross, *Spectrochimica Acta* 18 (1962) 225.
- [22] K. Nakamoto, *Infrared and Raman Spectra of Inorganic and Coordination Compounds*, Vol. 5, John Wiley & Sons, Toronto, 1986.
- [23] J. R. Stevens, P. Jacobsson, *Can. J. Chem.* 69 (1991) 1980.
- [24] A. Ferry, P. Jacobsson, J. D. van Heumen, J. R. Stevens, *Polymer* 37 (5) (1996) 737.

- [25] W. Wiczorek, A. Zalewska, D. Raducha, Z. Florjanczyk, J. R. Stevens, A. Ferry, P. Jacobson, *Macromolecules* 29 (1) (1996) 143.
- [26] L. Ducasse, M. Dussauze, J. Grodin, J.-C. Lassegues, C. Naudir, L. Servant, *Phys. Chem. Chem. Phys.* 5 (2003) 567.
- [27] J. Grodin, L. Ducasse, J. L. Bruneel, L. Servant, J. C. Lassegues, *Solid State Ionics*, 166 (2004) 441.
- [28] X. Huang, T. Ren, L. Tian, L. Hong, W. Zhun, X. Tang, *J. Materials Science* 39 (2004) 1221.
- [29] M. Marcinek, M. Ciosek, G. Zukowska, W. Wiczorek, K. R. Jeffrey, *Solid State Ionics* 176 (2005) 367.
- [30] M. H. Brooker, A. S. Quist, G. E. Boyd, *Chemical Physics Letters*, 9 (3) (1971) 242.
- [31] P. G. Bruce, C. A. Vincent, *Faraday Trans.* 89 (1993) 3187.
- [32] G. Petersen, A. Brodin, L. M. Torell, *Solid State Ionics*, 72 (1994) 165.
- [33] A Bernson, J. Lindgren, *Solid State Ionics*, 60 (1993) 31.
- [34] G. Petersen, L. M. Torell, S. Panero, B. Scrosati, C. J. R. Silva, M. J. Smith, *Solid State Ionics*, 60 (1993) 55.



(a)



(b)

Figure 1. Curve-fitting results of selected $d\text{-U}(2000)_n\text{LiClO}_4$ di-ureasils in the $\nu_1(\text{ClO}_4)$ region. The frequencies indicated represent the average value of the frequencies of all the samples considered.

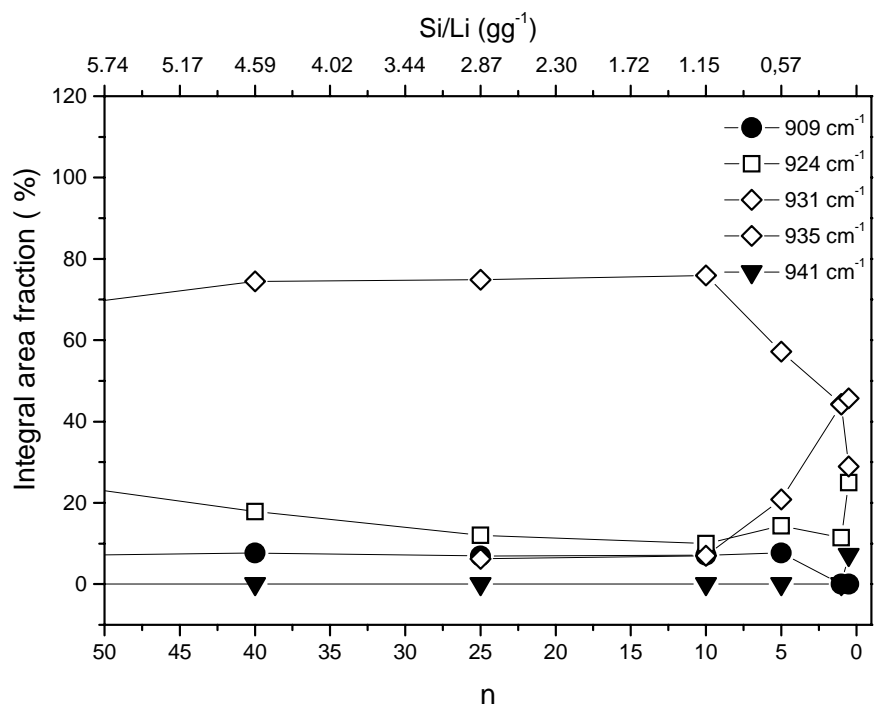


Figure 2. Variation of the integral area fraction of the isolated components with composition of of d-U(2000)_nLiClO₄ di-ureasils in the FT-Raman ν_1 ClO₄ region.

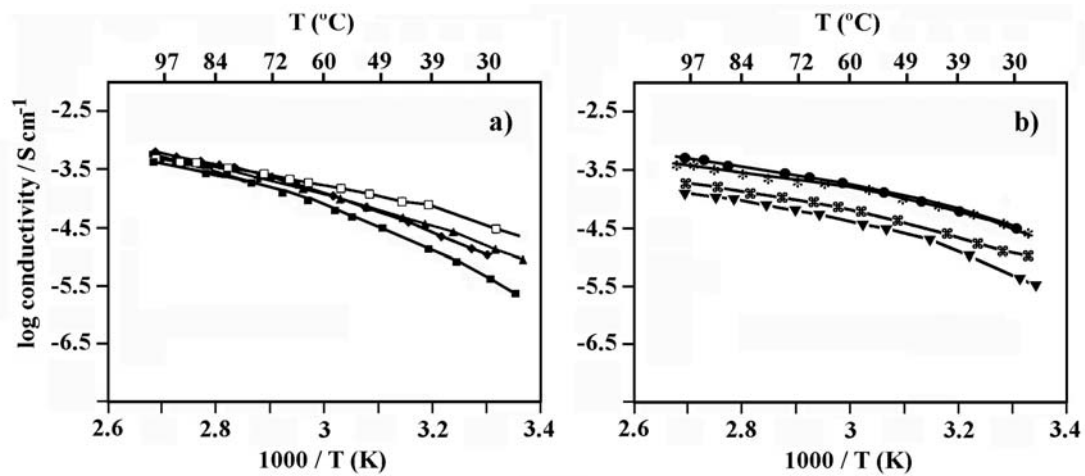


Figure 3(a) and (b). Variation of conductivity of selected $d(U2000)_nLiClO_4$ electrolyte compositions with temperature ($n = 5 \nu, 8 \upsilon, 10 \sigma, 20 \square, 30 *, 40 \lambda, 60 \times$ and 80τ).

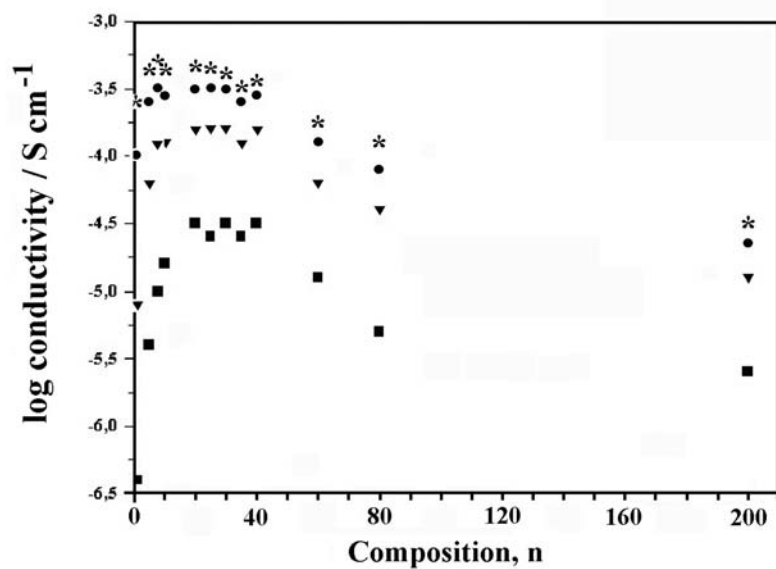


Figure 4. Isothermal variation of conductivity at $30 \nu, 60 \sigma, 80 \lambda, 90 *$ °C of $d(U2000)_nLiClO_4$ electrolytes.

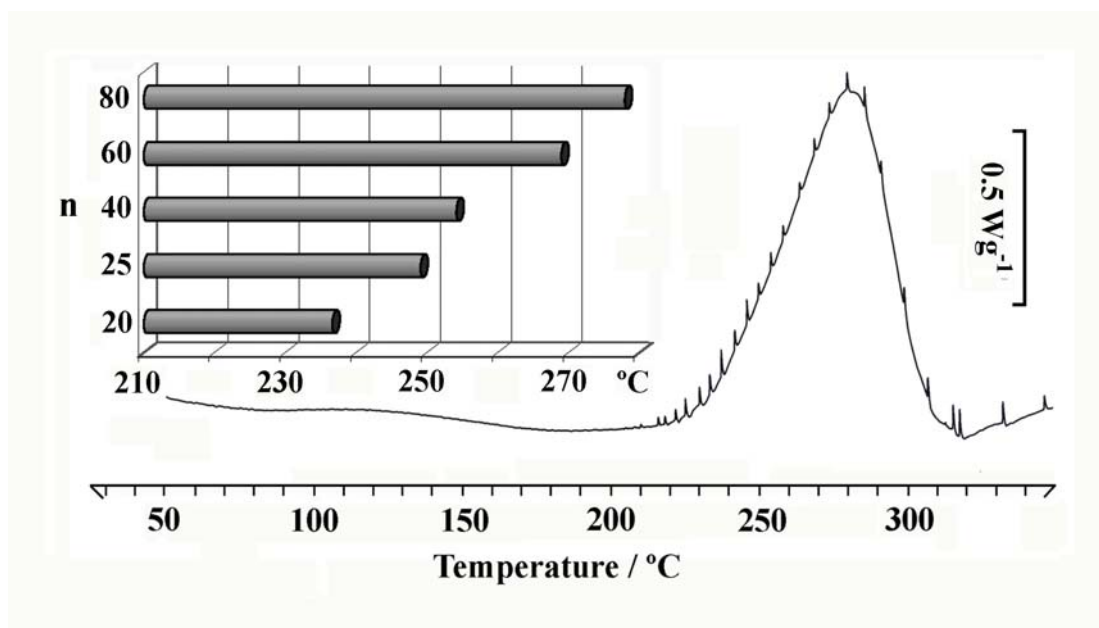


Figure 5. Onset of degradation temperatures of selected electrolyte compositions. Inset illustrates thermogram of $d(U2000)_{20}LiClO_4$.

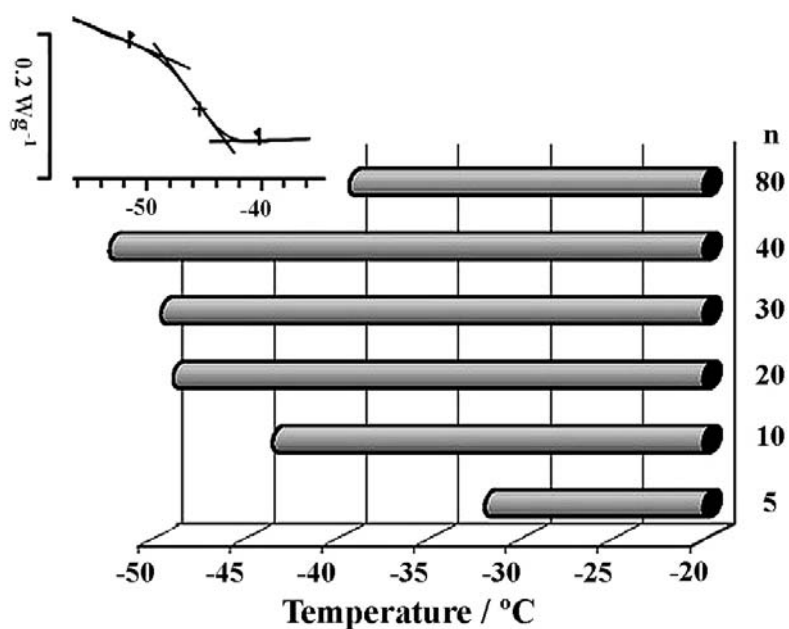


Figure 6. Extrapolated onset of glass transition temperatures of electrolyte compositions. Inset illustrates thermogram of $d(U2000)_{25}LiClO_4$.

Table 1, Relevant details of the synthetic procedure of the d-U(2000)_nLiClO₄ di-ureasils.

d-U(2000) _n LiClO ₄			
		Step 1	Step 2
V (Jeffamine)/g		2.0	
V(ICPTES)/ μl		494	
V(THF)/ml		10	
V(CH ₃ CH ₂ OH)/ μl		-	466
V(H ₂ O)/μl		-	54
n = O/Li ⁺ (molmol ⁻¹)	m(LiClO ₄) (g)	Si/Li ⁺ (molmol ⁻¹)	Si/Li ⁺ (gg ⁻¹)
∞	-	-	-
200	0.0215	9,8765	22.9642
80	0,05386	3,9506	9,1857
60	0,07181	2,9630	6,8893
40	0.1077	1.9753	4.5928
35	0.1231	1.7284	4.0187
30	0.1436	1.4815	3.4446
25	0.1724	1.2346	2.8705
20	0.2154	0.9876	2.2964
15	0.2872	0.7407	1.7223
10	0.4309	0.4938	1.1482
8	0.5386	0.3951	0.9185
5	0.8617	0.2469	0.5741
1	4.3088	0.0494	0.1148
0.5	8.6176	0.0247	0.0574

Table 2 - Composition dependence of the integral area fraction of the resolved components of d-U(2000)_nLiClO₄ di-ureasils in the FT-Raman ν_1 ClO₄ region.

n	Peak Position (cm ⁻¹)					Integrated área (%)				
	I	II	III	IV	V	I	II	III	IV	V
40	909	924	930	-	-	7.70	17.82	74.48	-	-
25	909	924	930	935	-	6.90	12.00	74.87	6.22	-
10	909	924	930	935	-	7.12	9,99	75,91	7.12	-
5	910	925	931	935	-	7.65	14.32	57.18	20.84	-
1	-	924	932	936	-	-	11.45	44.34	44.20	-
0,5	-	925	931	935	941	-	18.12	28.96	45.7	7.2